Measurement of the Top Pair Production Cross Section in the Lepton + Jets Channel Using a Jet Flavor Discriminant

T. Aaltonen,[21] B. Álvarez González[w],[9] S. Amerio,[41] D. Amidei,[32] A. Anastassov,[36] A. Annovi,[17] J. Antos,[12] G. Apollinari,[15] J.A. Appel,[15] A. Apresyan,[46] T. Arisawa,[56] A. Artikov,[13] J. Asaadi,[51] W. Ashmanskas,[15] B. Auerbach,[59] A. Aurisano,[51] F. Azfar,[40] W. Badgett,[15] A. Barbaro-Galtieri,[26] V.E. Barnes,[46] B.A. Barnett,[23] P. Barria[dd],[44] P. Bartos,[12] M. Bauce[bb],[41] G. Bauer,[30] F. Bedeschi,[44] D. Beecher,[28] S. Behari,[23] G. Bellettini[cc],[44] J. Bellinger,[58] D. Benjamin,[14] A. Beretvas,[15] A. Bhatti,[48] M. Binkley*,[15] D. Bisello[bb],[41] I. Bizjak[hh],[28] K.R. Bland,[5] B. Blumenfeld,[23] A. Bocci,[14] A. Bodek,[47] D. Bortoletto,[46] J. Boudreau,[45] A. Boveia,[11] B. Brau[a],[15] L. Brigliadori[aa],[6] A. Brisuda,[12] C. Bromberg,[33] E. Brucken,[21] M. Bucciantonio[cc],[44] J. Budagov,[13] H.S. Budd,[47] S. Budd,[22] K. Burkett,[15] G. Busetto[bb],[41] P. Bussey,[19] A. Buzatu,[31] C. Calancha,[29] S. Camarda,[4] M. Campanelli,[33] M. Campbell,[32] F. Canelli[11],[15] A. Canepa,[43] B. Carls,[22] D. Carlsmith,[58] R. Carosi,[44] S. Carrillo[k],[16] S. Carron,[15] B. Casal,[9] M. Casarsa,[15] A. Castro[aa],[6] P. Catastini,[15] D. Cauz,[52] V. Cavaliere[cc],[44] M. Cavalli-Sforza,[4] A. Cerri[f],[26] L. Cerrito[q],[28] Y.C. Chen,[1] M. Chertok,[7] G. Chiarelli,[44] G. Chlachidze,[15] F. Chlebana,[15] K. Cho,[25] D. Chokheli,[13] J.P. Chou,[20] W.H. Chung,[58] Y.S. Chung,[47] C.I. Ciobanu,[42] M.A. Ciocci[dd],[44] A. Clark,[18] G. Compostella[bb],[41] M.E. Convery,[15] J. Conway,[7] M.Corbo,[42] M. Cordelli,[17] C.A. Cox,[7] D.J. Cox,[7] F. Crescioli[cc],[44] C. Cuenca Almenar,[59] J. Cuevas[w],[9] R. Culbertson,[15] D. Dagenhart,[15] N. d'Ascenzo[u],[42] M. Datta,[15] P. de Barbaro,[47] S. De Cecco,[49] G. De Lorenzo,[4] M. Dell'Orso[cc],[44] C. Deluca,[4] L. Demortier,[48] J. Deng[c],[14] M. Deninno,[6] F. Devoto,[21] M. d'Errico[bb],[41] A. Di Canto[cc],[44] B. Di Ruzza,[44] J.R. Dittmann,[5] M. D'Onofrio,[27] S. Donati[cc],[44] P. Dong,[15] M. Dorigo,[52] T. Dorigo,[41] K. Ebina,[56] A. Elagin,[51] A. Eppig,[32] R. Erbacher,[7] D. Errede,[22] S. Errede,[22] N. Ershaidat[z],[42] R. Eusebi,[51] H.C. Fang,[26] S. Farrington,[40] M. Feindt,[24] J.P. Fernandez,[29] C. Ferrazza[ee],[44] R. Field,[16] G. Flanagan[s],[46] R. Forrest,[7] M.J. Frank,[5] M. Franklin,[20] J.C. Freeman,[15] Y. Funakoshi,[56] I. Furic,[16] M. Gallinaro,[48] J. Galyardt,[10] J.E. Garcia,[18] A.F. Garfinkel,[46] P. Garosi[dd],[44] H. Gerberich,[22] E. Gerchtein,[15] S. Giagu[ff],[49] V. Giakoumopoulou,[3] P. Giannetti,[44] K. Gibson,[45] C.M. Ginsburg,[15] N. Giokaris,[3] P. Giromini,[17] M. Giunta,[44] G. Giurgiu,[23] V. Glagolev,[13] D. Glenzinski,[15] M. Gold,[35] D. Goldin,[51] N. Goldschmidt,[16] A. Golossanov,[15] G. Gomez,[9] G. Gomez-Ceballos,[30] M. Goncharov,[30] O. González,[29] I. Gorelov,[35] A.T. Goshaw,[14] K. Goulianos,[48] S. Grinstein,[4] C. Grosso-Pilcher,[11] R.C. Group[55],[15] J. Guimaraes da Costa,[20] Z. Gunay-Unalan,[33] C. Haber,[26] S.R. Hahn,[15] E. Halkiadakis,[50] A. Hamaguchi,[39] J.Y. Han,[47] F. Happacher,[17] K. Hara,[53] D. Hare,[50] M. Hare,[54] R.F. Harr,[57] K. Hatakeyama,[5] C. Hays,[40] M. Heck,[24] J. Heinrich,[43] M. Herndon,[58] S. Hewamanage,[5] D. Hidas,[50] A. Hocker,[15] W. Hopkins[g],[15] D. Horn,[24] S. Hou,[1] R.E. Hughes,[37] M. Hurwitz,[11] U. Husemann,[59] N. Hussain,[31] M. Hussein,[33] J. Huston,[33] G. Introzzi,[44] M. Iori[ff],[49] A. Ivanov[o],[7] E. James,[15] D. Jang,[10] B. Jayatilaka,[14] E.J. Jeon,[25] M.K. Jha,[6] S. Jindariani,[15] W. Johnson,[7] M. Jones,[46] K.K. Joo,[25] S.Y. Jun,[10] T.R. Junk,[15] T. Kamon,[51] P.E. Karchin,[57] A. Kasmi,[5] Y. Kato[n],[39] W. Ketchum,[11] J. Keung,[43] V. Khotilovich,[51] B. Kilminster,[15] D.H. Kim,[25] H.S. Kim,[25] H.W. Kim,[25] J.E. Kim,[25] M.J. Kim,[17] S.B. Kim,[25] S.H. Kim,[53] Y.K. Kim,[11] N. Kimura,[56] M. Kirby,[15] S. Klimenko,[16] K. Kondo,[56] D.J. Kong,[25] J. Konigsberg,[16] A.V. Kotwal,[14] M. Kreps,[24] J. Kroll,[43] D. Krop,[11] N. Krumnack[l],[5] M. Kruse,[14] V. Krutelyov[d],[51] T. Kuhr,[24] M. Kurata,[53] S. Kwang,[11] A.T. Laasanen,[46] S. Lami,[44] S. Lammel,[15] M. Lancaster,[28] R.L. Lander,[7] K. Lannon[v],[37] A. Lath,[50] G. Latino[cc],[44] T. LeCompte,[2] E. Lee,[51] H.S. Lee,[11] J.S. Lee,[25] S.W. Lee[x],[51] S. Leo[cc],[44] S. Leone,[44] J.D. Lewis,[15] A. Limosani[r],[14] C.-J. Lin,[26] J. Linacre,[40] M. Lindgren,[15] E. Lipeles,[43] A. Lister,[18] D.O. Litvintsev,[15] C. Liu,[45] Q. Liu,[46] T. Liu,[15] S. Lockwitz,[59] N.S. Lockyer,[43] A. Loginov,[59] D. Lucchesi[bb],[41] J. Lueck,[24] P. Lujan,[26] P. Lukens,[15] G. Lungu,[48] J. Lys,[26] R. Lysak,[12] R. Madrak,[15] K. Maeshima,[15] K. Makhoul,[30] P. Maksimovic,[23] S. Malik,[48] G. Manca[b],[27] M.L. Mangano[ii],[15] A. Manousakis-Katsikakis,[3] F. Margaroli,[46] C. Marino,[24] M. Martínez,[4] R. Martínez-Ballarín,[29] P. Mastrandrea,[49] M. Mathis,[23] M.E. Mattson,[57] P. Mazzanti,[6] K.S. McFarland,[47] P. McIntyre,[51] R. McNulty[i],[27] A. Mehta,[27] P. Mehtala,[21] A. Menzione,[44] C. Mesropian,[48] T. Miao,[15] D. Mietlicki,[32] A. Mitra,[1] H. Miyake,[53] S. Moed,[20] N. Moggi,[6] M.N. Mondragon[k],[15] C.S. Moon,[25] R. Moore,[15] M.J. Morello,[15] J. Morlock,[24] P. Movilla Fernandez,[15] A. Mukherjee,[15] Th. Muller,[24] P. Murat,[15] M. Mussini[aa],[6] J. Nachtman[m],[15] Y. Nagai,[53] J. Naganoma,[56] I. Nakano,[38] A. Napier,[54] J. Nett,[51] C. Neu,[55] M.S. Neubauer,[22] J. Nielsen[e],[26] L. Nodulman,[2] O. Norniella,[22] E. Nurse,[28] L. Oakes,[40] S.H. Oh,[14] Y.D. Oh,[25] I. Oksuzian,[55] T. Okusawa,[39] R. Orava,[21] L. Ortolan,[4] S. Pagan Griso[bb],[41] C. Pagliarone,[52] E. Palencia[f],[9] V. Papadimitriou,[15] A.A. Paramonov,[2] J. Patrick,[15] G. Pauletta[gg],[52] M. Paulini,[10] C. Paus,[30] D.E. Pellett,[7] A. Penzo,[52] T.J. Phillips,[14] G. Piacentino,[44] E. Pianori,[43] J. Pilot,[37] K. Pitts,[22] C. Plager,[8] L. Pondrom,[58] K. Potamianos,[46] O. Poukhov*,[13] F. Prokoshin[y],[13]

A. Pronko,[15] F. Ptohos[h],[17] E. Pueschel,[10] G. Punzi[cc],[44] J. Pursley,[58] A. Rahaman,[45] V. Ramakrishnan,[58] N. Ranjan,[46] I. Redondo,[29] P. Renton,[40] M. Rescigno,[49] F. Rimondi[aa],[6] L. Ristori[45],[15] A. Robson,[19] T. Rodrigo,[9] T. Rodriguez,[43] E. Rogers,[22] S. Rolli,[54] R. Roser,[15] M. Rossi,[52] F. Rubbo,[15] F. Ruffini[dd],[44] A. Ruiz,[9] J. Russ,[10] V. Rusu,[15] A. Safonov,[51] W.K. Sakumoto,[47] Y. Sakurai,[56] L. Santi[gg],[52] L. Sartori,[44] K. Sato,[53] V. Saveliev[u],[42] A. Savoy-Navarro,[42] P. Schlabach,[15] A. Schmidt,[24] E.E. Schmidt,[15] M.P. Schmidt[*],[59] M. Schmitt,[36] T. Schwarz,[7] L. Scodellaro,[9] A. Scribano[dd],[44] F. Scuri,[44] A. Sedov,[46] S. Seidel,[35] Y. Seiya,[39] A. Semenov,[13] E. Sexton-Kennedy,[15] F. Sforza[cc],[44] A. Sfyrla,[22] S.Z. Shalhout,[7] T. Shears,[27] P.F. Shepard,[45] M. Shimojima[t],[53] S. Shiraishi,[11] M. Shochet,[11] I. Shreyber,[34] A. Simonenko,[13] P. Sinervo,[31] A. Sissakian[*],[13] K. Sliwa,[54] J.R. Smith,[7] F.D. Snider,[15] A. Soha,[15] S. Somalwar,[50] V. Sorin,[4] P. Squillacioti,[15] M. Stancari,[15] M. Stanitzki,[59] R. St. Denis,[19] B. Stelzer,[31] O. Stelzer-Chilton,[31] D. Stentz,[36] J. Strologas,[35] G.L. Strycker,[32] Y. Sudo,[53] A. Sukhanov,[16] I. Suslov,[13] K. Takemasa,[53] Y. Takeuchi,[53] J. Tang,[11] M. Tecchio,[32] P.K. Teng,[1] J. Thom[g],[15] J. Thome,[10] G.A. Thompson,[22] E. Thomson,[43] P. Ttito-Guzmán,[29] S. Tkaczyk,[15] D. Toback,[51] S. Tokar,[12] K. Tollefson,[33] T. Tomura,[53] D. Tonelli,[15] S. Torre,[17] D. Torretta,[15] P. Totaro,[41] M. Trovato[ee],[44] Y. Tu,[43] F. Ukegawa,[53] S. Uozumi,[25] A. Varganov,[32] F. Vázquez[k],[16] G. Velev,[15] C. Vellidis,[3] M. Vidal,[29] I. Vila,[9] R. Vilar,[9] J. Vizán,[9] M. Vogel,[35] G. Volpi[cc],[44] P. Wagner,[43] R.L. Wagner,[15] T. Wakisaka,[39] R. Wallny,[8] S.M. Wang,[1] A. Warburton,[31] D. Waters,[28] M. Weinberger,[51] W.C. Wester III,[15] B. Whitehouse,[54] D. Whiteson[c],[43] A.B. Wicklund,[2] E. Wicklund,[15] S. Wilbur,[11] F. Wick,[24] H.H. Williams,[43] J.S. Wilson,[37] P. Wilson,[15] B.L. Winer,[37] P. Wittich[g],[15] S. Wolbers,[15] H. Wolfe,[37] T. Wright,[32] X. Wu,[18] Z. Wu,[5] K. Yamamoto,[39] J. Yamaoka,[14] T. Yang,[15] U.K. Yang[p],[11] Y.C. Yang,[25] W.-M. Yao,[26] G.P. Yeh,[15] K. Yi[m],[15] J. Yoh,[15] K. Yorita,[56] T. Yoshida[j],[39] G.B. Yu,[14] I. Yu,[25] S.S. Yu,[15] J.C. Yun,[15] A. Zanetti,[52] Y. Zeng,[14] and S. Zucchelli[aa6]

(CDF Collaboration[†])

[1]*Institute of Physics, Academia Sinica, Taipei, Taiwan 11529, Republic of China*
[2]*Argonne National Laboratory, Argonne, Illinois 60439, USA*
[3]*University of Athens, 157 71 Athens, Greece*
[4]*Institut de Fisica d'Altes Energies, ICREA, Universitat Autonoma de Barcelona, E-08193, Bellaterra (Barcelona), Spain*
[5]*Baylor University, Waco, Texas 76798, USA*
[6]*Istituto Nazionale di Fisica Nucleare Bologna, [aa]University of Bologna, I-40127 Bologna, Italy*
[7]*University of California, Davis, Davis, California 95616, USA*
[8]*University of California, Los Angeles, Los Angeles, California 90024, USA*
[9]*Instituto de Fisica de Cantabria, CSIC-University of Cantabria, 39005 Santander, Spain*
[10]*Carnegie Mellon University, Pittsburgh, Pennsylvania 15213, USA*
[11]*Enrico Fermi Institute, University of Chicago, Chicago, Illinois 60637, USA*
[12]*Comenius University, 842 48 Bratislava, Slovakia; Institute of Experimental Physics, 040 01 Kosice, Slovakia*
[13]*Joint Institute for Nuclear Research, RU-141980 Dubna, Russia*
[14]*Duke University, Durham, North Carolina 27708, USA*
[15]*Fermi National Accelerator Laboratory, Batavia, Illinois 60510, USA*
[16]*University of Florida, Gainesville, Florida 32611, USA*
[17]*Laboratori Nazionali di Frascati, Istituto Nazionale di Fisica Nucleare, I-00044 Frascati, Italy*
[18]*University of Geneva, CH-1211 Geneva 4, Switzerland*
[19]*Glasgow University, Glasgow G12 8QQ, United Kingdom*
[20]*Harvard University, Cambridge, Massachusetts 02138, USA*
[21]*Division of High Energy Physics, Department of Physics,*
University of Helsinki and Helsinki Institute of Physics, FIN-00014, Helsinki, Finland
[22]*University of Illinois, Urbana, Illinois 61801, USA*
[23]*The Johns Hopkins University, Baltimore, Maryland 21218, USA*
[24]*Institut für Experimentelle Kernphysik, Karlsruhe Institute of Technology, D-76131 Karlsruhe, Germany*
[25]*Center for High Energy Physics: Kyungpook National University,*
Daegu 702-701, Korea; Seoul National University, Seoul 151-742,
Korea; Sungkyunkwan University, Suwon 440-746,
Korea; Korea Institute of Science and Technology Information,
Daejeon 305-806, Korea; Chonnam National University, Gwangju 500-757,
Korea; Chonbuk National University, Jeonju 561-756, Korea
[26]*Ernest Orlando Lawrence Berkeley National Laboratory, Berkeley, California 94720, USA*
[27]*University of Liverpool, Liverpool L69 7ZE, United Kingdom*
[28]*University College London, London WC1E 6BT, United Kingdom*
[29]*Centro de Investigaciones Energeticas Medioambientales y Tecnologicas, E-28040 Madrid, Spain*
[30]*Massachusetts Institute of Technology, Cambridge, Massachusetts 02139, USA*

[31] Institute of Particle Physics: McGill University, Montréal, Québec, Canada H3A 2T8; Simon Fraser University, Burnaby, British Columbia, Canada V5A 1S6; University of Toronto, Toronto, Ontario, Canada M5S 1A7; and TRIUMF, Vancouver, British Columbia, Canada V6T 2A3
[32] University of Michigan, Ann Arbor, Michigan 48109, USA
[33] Michigan State University, East Lansing, Michigan 48824, USA
[34] Institution for Theoretical and Experimental Physics, ITEP, Moscow 117259, Russia
[35] University of New Mexico, Albuquerque, New Mexico 87131, USA
[36] Northwestern University, Evanston, Illinois 60208, USA
[37] The Ohio State University, Columbus, Ohio 43210, USA
[38] Okayama University, Okayama 700-8530, Japan
[39] Osaka City University, Osaka 588, Japan
[40] University of Oxford, Oxford OX1 3RH, United Kingdom
[41] Istituto Nazionale di Fisica Nucleare, Sezione di Padova-Trento, [bb] University of Padova, I-35131 Padova, Italy
[42] LPNHE, Universite Pierre et Marie Curie/IN2P3-CNRS, UMR7585, Paris, F-75252 France
[43] University of Pennsylvania, Philadelphia, Pennsylvania 19104, USA
[44] Istituto Nazionale di Fisica Nucleare Pisa, [cc] University of Pisa, [dd] University of Siena and [ee] Scuola Normale Superiore, I-56127 Pisa, Italy
[45] University of Pittsburgh, Pittsburgh, Pennsylvania 15260, USA
[46] Purdue University, West Lafayette, Indiana 47907, USA
[47] University of Rochester, Rochester, New York 14627, USA
[48] The Rockefeller University, New York, New York 10065, USA
[49] Istituto Nazionale di Fisica Nucleare, Sezione di Roma 1, [ff] Sapienza Università di Roma, I-00185 Roma, Italy
[50] Rutgers University, Piscataway, New Jersey 08855, USA
[51] Texas A&M University, College Station, Texas 77843, USA
[52] Istituto Nazionale di Fisica Nucleare Trieste/Udine, I-34100 Trieste, [gg] University of Trieste/Udine, I-33100 Udine, Italy
[53] University of Tsukuba, Tsukuba, Ibaraki 305, Japan
[54] Tufts University, Medford, Massachusetts 02155, USA
[55] University of Virginia, Charlottesville, VA 22906, USA
[56] Waseda University, Tokyo 169, Japan
[57] Wayne State University, Detroit, Michigan 48201, USA
[58] University of Wisconsin, Madison, Wisconsin 53706, USA
[59] Yale University, New Haven, Connecticut 06520, USA

We present a new method to measure the top quark pair production cross section and the background rates with data corresponding to an integrated luminosity of 2.7 fb^{-1} from $p\bar{p}$ collisions at $\sqrt{s}$ =1.96 TeV collected with the CDF II Detector. We select events with a single electron or muon candidate, missing transverse energy, and at least one b-tagged jet. We perform a simultaneous fit to a jet flavor discriminant across nine samples defined by the number of jets and b-tags. An advantage of this approach is that many systematic uncertainties are measured *in situ* and inversely scale with integrated luminosity. We measure a top cross section of $\sigma_{t\bar{t}} = 7.64 \pm 0.57$ (stat + syst) ± 0.45 (luminosity) pb.

PACS numbers: 14.65.Ha, 13.87.-a, 13.85.Qk

Since its discovery in 1995 [1, 2], much has been learned about the top quark through analyses of $p\bar{p}$ collisions.

*Deceased
†With visitors from [a] University of Massachusetts Amherst, Amherst, Massachusetts 01003, [b] Istituto Nazionale di Fisica Nucleare, Sezione di Cagliari, 09042 Monserrato (Cagliari), Italy, [c] University of California Irvine, Irvine, CA 92697, [d] University of California Santa Barbara, Santa Barbara, CA 93106 [e] University of California Santa Cruz, Santa Cruz, CA 95064, [f] CERN,CH-1211 Geneva, Switzerland, [ii] CERN, PH-TH Geneva, Switzerland, [g] Cornell University, Ithaca, NY 14853, [h] University of Cyprus, Nicosia CY-1678, Cyprus, [i] University College Dublin, Dublin 4, Ireland, [j] University of Fukui, Fukui City, Fukui Prefecture, Japan 910-0017, [k] Universidad Iberoamericana, Mexico D.F., Mexico, [l] Iowa State University, Ames, IA 50011, [m] University of Iowa, Iowa City, IA 52242, [n] Kinki University, Higashi-Osaka City, Japan 577-8502, [o] Kansas State University, Manhattan, KS 66506, [p] University of Manchester, Manchester M13 9PL, England, [q] Queen Mary, University of London, London, E1 4NS, England, [r] University of Melbourne, Victoria 3010, Australia, [s] Muons, Inc., Batavia, IL 60510, [t] Nagasaki Institute of Applied Science, Nagasaki, Japan, [u] National Research Nuclear University, Moscow, Russia, [v] University of Notre Dame, Notre Dame, IN 46556, [w] Universidad de Oviedo, E-33007 Oviedo, Spain, [x] Texas Tech University, Lubbock, TX 79609, [y] Universidad Tecnica Federico Santa Maria, 110v Valparaiso, Chile, [z] Yarmouk University, Irbid 211-63, Jordan, [hh] On leave from J. Stefan Institute, Ljubljana, Slovenia,

Top quarks are produced in pairs through the strong interaction and each top quark decays dominantly to a W boson and a b quark, followed by the W decaying either to a pair of quarks (which form jets) or a lepton and a neutrino. This paper describes a measurement of the top-antitop pair production cross section, $\sigma_{t\bar{t}}$, in the $p\bar{p} \to t\bar{t} \to \ell\nu qq'b\bar{b}$ channel at a center-of-mass energy, $\sqrt{s} = 1.96$ TeV using a new methodology to constrain background contributions and systematic effects, resulting in an improved sensitivity.

The jets which originate from the bottom quarks in the final state provide an opportunity to select events which are more likely to have come from top quark decays than from other processes. A b-tagging algorithm takes advantage of the characteristics—largely the secondary vertex displaced from the primary vertex—that distinguish heavy flavor (HF) jets from charm and light flavor (LF) jets [3]. This algorithm allows us to reduce the backgrounds from W + jets processes, which can mimic the top decay signature, and was the basis for several previous measurements of the top cross section [4, 5].

While requiring the event to have at least one b-tagged jet reduces the backgrounds, it does not eliminate them. It is important to estimate the amount of W boson production with associated jets from heavy flavor, which is theoretically difficult and a source of systematic uncertainties for measurements of the cross section as well as the mass. Here we reduce this systematic uncertainty and constrain the W+HF background by performing a fit to the data which includes regions dominated by W + jets.

Since the b-tagging algorithm can incorrectly tag light flavor jets as b jets, it is advantageous to apply an additional discriminant to b-tagged jets to further separate processes with jets from bottom, charm, and light flavor. This flavor separator is a neural network whose output, on a statistical basis, discriminates between b-quark, c-quark, and light-flavor jets. The flavor separator uses 25 variables to output a single number indicating how likely a jet is a b jet, where the invariant mass of the secondary vertex has the most separation power. The flavor separator was calibrated using data control samples [6].

In this paper, we use a flavor separator for the first time in the measurement of the $t\bar{t}$ cross-section. In order to constrain the background contributions, we perform the fit to the flavor discriminant in nine samples defined by the number of jets, n_{jet} (1, 2, 3, 4, or ≥ 5), and number of b-tagged jets, n_{tag} (1 or ≥ 2). Events with one or two jets are dominated by W + jets, whereas events with three or more jets are largely $t\bar{t}$. Events with two b tags are dominated by $Wb\bar{b}$ and $t\bar{t}$, whereas events with a single b tag are predominantly W+charm and W+LF. Previous methods selected events with three or more jets in order to reduce the largest background from W + jets processes [4, 5, 7]. This new method instead constrains the background contribution of the W + jets processes in the region with three or more jets by measuring the contributions in the regions with one and two jets.

We use a data sample corresponding to 2.7 fb^{-1} of integrated luminosity, collected from February 2002 through April 2008 using the CDF II detector [8], an approximately cylindrically symmetric detector located at the Tevatron collider. CDF II is a general-purpose device; the central drift chamber provides charged-particle tracking, while the silicon system provides excellent vertex and impact parameter resolution, both of which are important for identifying bottom quarks. Electromagnetic and hadronic calorimeters are located outside the tracking chambers, and provide identification of electrons and jets. At the outermost layer of the detector sit the muon drift chambers which provide muon identification.

We select events with a W candidate decaying leptonically to either an electron or muon. We require at least one jet and exactly one lepton candidate both with transverse energy $E_T > 20$ GeV and pseudorapidity $|\eta| < 2.0$ [9]. We require that at least one jet is b-tagged, and that there is at least 20 GeV of missing transverse energy, $\not\!\!E_T$, in the event. To reduce QCD backgrounds, we require the transverse mass of the W, $m_T^W = \sqrt{2(p_T^\ell p_T^\nu - p_x^\ell p_x^\nu - p_y^\ell p_y^\nu)}$, to be at least 10 GeV/$c^2$ for muons, and at least 20 GeV/c^2 for electrons. Electron samples have a larger QCD background contamination than muon samples, so there we also require the $\not\!\!E_T$ to satisfy $\frac{\not\!\!E_T}{\sqrt{\vec{E}_T^{\,\rm uncl.} \cdot \hat{\not\!\!E}_T}} > -0.05\ m_T^W\ ({\rm inGeV/c^2}) + 3.5$, where the denominator is the square root of the amount of unclustered energy in the direction of the missing transverse energy [10].

In addition to QCD multi-jet processes, the final state in this analysis can be mimicked by several other processes. W + jets processes are by far the largest source of backgrounds. Single top production, di-boson production, and Z + jets processes — collectively referred to as electroweak (EW) processes — also contribute. All but the QCD multi-jet backgrounds are modeled with Monte Carlo simulations; the QCD backgrounds are estimated using a data-driven approach. Events that pass the selection criteria, though with the lepton candidate failing any two identification cuts, are mostly QCD multi-jet processes, and this sample is used to model the background from these QCD processes. The normalization of the QCD background is estimated from a fit to the missing E_T distribution for each sub-sample, without the missing E_T requirement.

Monte Carlo samples are employed to estimate acceptances for the signal and backgrounds, and to model relevant distributions used in the fits described below. All of the Monte Carlo samples employed were generated using either PYTHIA v6.216 [11] (the $t\bar{t}$ and diboson samples), MADGRAPH [12] (the single top sample), or ALPGEN v2.10′ [13] with generator-to-reconstructed-jet

matching [14, 15] and PYTHIA v6.326 for showering (the W + jets and Z + jets samples). The $t\bar{t}$ signal Monte Carlo sample was generated with the CTEQ5L [16] parton distribution functions (PDFs) assuming a top mass of $m_t = 175$ GeV/c^2. All samples are processed through a detailed simulation of the CDF II detector response, after which they are treated in the same manner as the data events. Each of the samples is divided based on the number of jets and b tags, and made into templates—binned distributions of the flavor separator output.

The measurement is accomplished as a fit of the flavor separator distribution performed simultaneously in the nine data sub-samples. Results are obtained by maximizing a binned Poisson likelihood which incorporates templates from each of the $t\bar{t}$, W + jets, electroweak, and QCD processes. The templates are combined after initializing them to the predicted yield for data corresponding to an integrated luminosity of 2.7 fb^{-1}, where the initialization factors are functions of cross sections, tagging efficiencies, and energy scales which are all parameters in the fit. The overall normalization of each template is floated in the fit — a single overall normalization factor is used for each process — and the primary result of the fit is a set of those normalizations: the $t\bar{t}$ cross section and relative normalizations, K_p, to the standard model expectations for W + jets, electroweak, and QCD components.

Template normalizations also include functions, $P_x(i, j, \xi_x)$, that parametrize the effect of a source of systematic uncertainty, x, in the sub-sample with $\mathrm{n}_{tag} = i$ and $\mathrm{n}_{jet} = j$, as a function of the relative shift, ξ_x, of quantity x, in units of the uncertainty on x. A separate function is employed for each process in each subsample for each source of systematic uncertainty; an example function is shown in Fig. 1. This leads to a total of 12 parameters in the fit—seven normalizations of the samples ($\sigma_{t\bar{t}}$, $K_{Wb\bar{b}}$, $K_{Wc\bar{c}}$, K_{Wc}, K_{W+LF}, K_{EW}, and K_{QCD}), and five systematic uncertainty parameters (ξ_{Btag}, ξ_{Mistag}, $\xi_{I/FSR}$, ξ_{Q^2}, ξ_{JES}).

Systematic uncertainties in this measurement can affect both the normalizations and the shapes of the templates. The rate uncertainties are naturally included in the fit via the $P_x(i, j, \xi_x)$ functions, and these systematic uncertainties are reflected by the total fit error. To account for each shape uncertainty, we generate an additional set of templates with the variable in question changed, re-run the fit, and take the difference in the result as the uncertainty.

We vary the b-tagging efficiency, mistag rate, and the jet energy calibration [17] by their uncertainties for all simulated samples. Initial- and final-state radiation (ISR/FSR) are processes in which gluons are radiated before or after the collision, respectively. The uncertainty arises due to ISR/FSR leading to a larger or smaller number of jets in the event. To account for this, we make additional sets of $t\bar{t}$ templates with more or less ISR and

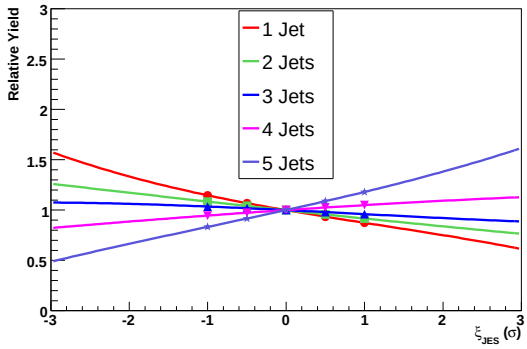

FIG. 1. (Color) The function which parameterizes the effect of the jet energy scale on the 1-tag templates of the $t\bar{t}$ sample. Each jet and tag bin for each process in each subsample has a different function for each source of systematic uncertainty. The x axis is in units of the systematic shift.

FSR as compared to the normal settings; the different settings are constrained by studies of Drell-Yan production [18]. The systematic uncertainty associated to the choice of the renormalization and factorization scales is estimated by varying these scales between half and twice their default values, as indicated in [13]. This variation also accounts for differences in ISR/FSR in W + jets processes.

The uncertainty due to the choice of the algorithm used to generate the parton shower was determined by comparing the results obtained using PYTHIA and HERWIG [19]. We account for uncertainties in our modeling of the QCD template shape by using electronlike signals associated with multiple tracks, rather than electrons that fail identification cuts, to make templates. The flavor separator has a correction factor applied to match its mistag rate to the one observed in data; to account for this uncertainty, we examine templates without this factor applied. The models describing color reconnection—i.e., the QCD cross-talk between the decay products of the top quarks—are not known precisely, so we account for this uncertainty by comparing two different models. We take an uncertainty of 0.6% on the top cross section due to the PDFs, and an uncertainty of 0.5% due to the beam position and lepton identification efficiency. We take a conservative 2% uncertainty due to the PDFs on the W + jets results. The measured luminosity has an uncertainty of 5.9%.

The total normalizations of the $t\bar{t}$ and $Wb\bar{b}$ components

in the fit are given by

$$N^{pred}_{t\bar{t}}(i,j) = \sigma_{t\bar{t}} \cdot L \cdot F^{MC}_{t\bar{t}}(i,j) \cdot P_{I/FSR}(i,j,\xi_{I/FSR}) \cdot P_{Btag}(i,j,\xi_{Btag}) \cdot P_{Mistag}(i,j,\xi_{Mistag}) \cdot P_{JES}(i,j,\xi_{JES}) \quad (1)$$

$$N^{pred}_{Wb\bar{b}}(i,j) = K_{Wb\bar{b}} \cdot \sigma^{MC}_{Wb\bar{b}} \cdot L \cdot S_{\sigma_W} \cdot F^{MC}_{Wb\bar{b}}(i,j) \cdot P_{Btag}(i,j,\xi_{Btag}) \cdot P_{Mistag}(i,j,\xi_{Mistag}) \cdot P_{JES}(i,j,\xi_{JES}) \cdot P_{Q^2}(i,j,\xi_{Q^2}) \quad (2)$$

where $\sigma_{t\bar{t}}$ is the cross section and $K_{Wb\bar{b}}$ is the relative normalization factor; σ^{MC}_x is the cross section from Monte Carlo simulations; $L = \int \mathcal{L} dt$ is the integrated luminosity; $F^{MC}_x(i,j)$ is the Monte Carlo prediction for the fraction of events with i b tags and j jets, including reconstruction and selection efficiencies; S_{σ_W} is a factor of 1.54 obtained from the ratio of the measured W + jets cross section [20] to the ALPGEN-prediction cross section —this is necessary due to ALPGEN being a leading-order event generator; and $P_x(i,j,\xi_x)$ are functions for each source of systematic uncertainty, x. Normalizations of the other five samples are obtained in a similar manner. For reference and easier comparison to other measurements, the cross sections for $K = 1$ are calculated from ALPGEN as 2744.1 pb for W+LF, 31.9 pb for Wc, 13.1 pb for $Wc\bar{c}$, and 6.8 pb for $Wb\bar{b}$.

The data and best fit to the flavor separator distribution are shown in Fig. 2. The $t\bar{t}$ production cross section is found to be $\sigma_{t\bar{t}} = 7.64^{+0.57}_{-0.54}$ pb, and relative normalization factors are $K_{Wb\bar{b}} = 1.39^{+0.28}_{-0.22}$, $K_{Wc\bar{c}} = 0.83^{+0.90}_{-0.71}$, $K_{Wc} = 1.68^{+0.34}_{-0.32}$, $K_{W+LF} = 0.98^{+0.34}_{-0.25}$, $K_{EW} = 1.10^{+0.10}_{-0.10}$, and $K_{QCD} = 0.82^{+0.26}_{-0.26}$. These results include statistical and systematic uncertainties, but do not include an uncertainty due to the luminosity. The top cross section we measure is consistent with theoretical predictions [21–24], and the values of the relative normalizations are consistent with what is expected from the theoretical uncertainty of the leading-order cross sections used by the Monte Carlo simulation generators [13, 14].

In order to evaluate the performance of this new method, we have compared the estimates of the systematic uncertainties on the top cross section with the previous method of background estimation [7], though as applied to the same integrated luminosity. A summary of these comparisons is shown in Table I. The total uncertainty drops from 0.84 pb to 0.73 pb, which is a 13% improvement. However, the previous result developed a normalization to the Z cross section to reduce the luminosity uncertainty dramatically, and this method can be extended in the future to include that improvement. Therefore, upon excluding the luminosity uncertainty in order to better compare the methods, the uncertainty drops from 0.72 pb to 0.57 pb for a 21% improvement.

In summary, we measured the top pair production cross section using a novel method for estimating background contributions with CDF II data corresponding to an integrated luminosity of 2.7 fb^{-1}. The cross section we measure, 7.64 ± 0.57 (stat + syst) ± 0.45 (luminosity), is consistent with the standard model next-to-leading order theoretical calculation [22], and the background contributions are consistent with other predictions [7]. Compared to the previous method of background estimation, using b-tagging, this new method improves the precision on the top quark pair production cross section by 21%, excluding luminosity uncertainties.

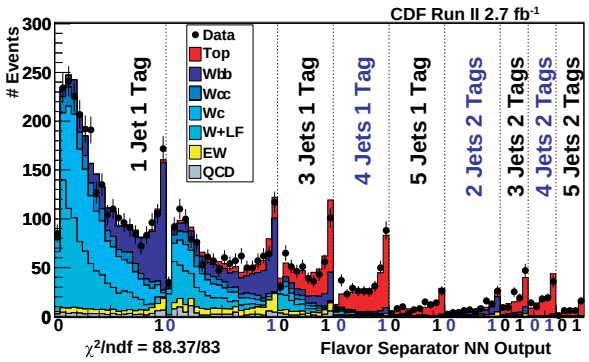

FIG. 2. (Color) The data and best fit for the flavor separator distribution for samples defined by the number of jets and number of tags. The legend is located in the "2 Jets 1 Tag" bin. Note that the flavor separator distribution is divided into fewer bins for samples with fewer events. For samples with two or more tags, we show the average of the flavor separator output from the two highest-p_T tagged jets.

TABLE I. Comparison of systematic uncertainties between this result and the previous method of background estimation [7].

Uncertainty	Previous Method	This Result
Statistical	0.36 pb	0.33 pb
HF K-Factor	0.27 pb	Inc in stat
Q^2	N/A	0.21 pb
B Tagging	0.39 pb	0.23 pb
Mistags	0.17 pb	0.08 pb
JES	0.29 pb	0.29 pb
ISR/FSR	0.06 pb	0.01 pb
Parton Showering	0.21 pb	0.11 pb
QCD Shape	0.06 pb	0.01 pb
Flavor Separator Correction	N/A	0.10 pb
Color Reconnection	N/A	0.03 pb
PDF	0.04 pb	0.05 pb
Lepton ID / trigger	0.04 pb	0.05 pb
Z0	0.02 pb	0.02 pb
Sub-Total	0.72 pb	0.57 pb
Luminosity	0.43 pb	0.45 pb
Total	0.84 pb	0.73 pb

We thank the Fermilab staff and the technical staffs of the participating institutions for their vital contributions. This work was supported by the U.S. Department of Energy and National Science Foundation; the Italian Istituto Nazionale di Fisica Nucleare; the Ministry of Education, Culture, Sports, Science and Technology of Japan; the Natural Sciences and Engineering Research Council of Canada; the National Science Council of the Republic of China; the Swiss National Science Foundation; the A.P. Sloan Foundation; the Bundesministerium für Bildung und Forschung, Germany; the Korean World Class University Program, the National Research Foundation of Korea; the Science and Technology Facilities Council and the Royal Society, UK; the Institut National de Physique Nucleaire et Physique des Particules/CNRS; the Russian Foundation for Basic Research; the Ministerio de Ciencia e Innovación, and Programa Consolider-Ingenio 2010, Spain; the Slovak R&D Agency; and the Academy of Finland.

[1] F. Abe *et al.* (CDF Collaboration), Phys. Rev. Lett. **74** (1995), 2626–2631.
[2] S. Abachi *et al.* (DØ Collaboration), Phys. Rev. Lett. **74** (1995), 2632–2637.
[3] D. Acosta *et al.* (CDF Collaboration), Phys. Rev. D **71** (2005), 052003.
[4] A. Abulencia *et al.* (CDF Collaboration), Phys. Rev. Lett. **97** (2006), no. 8, 082004.
[5] V. M. Abazov *et al.* (DØ Collaboration), Phys. Rev. Lett. **100** (2008), no. 19, 192003.
[6] S. Richter, Ph.D. thesis, Universität Karlsruhe, 2007.
[7] T. Aaltonen *et al.* (CDF Collaboration), Phys. Rev. Lett. **105** (2010), 012001.
[8] D. Acosta *et al.* (CDF Collaboration), Phys. Rev. D **71** (2005), 032001.
[9] We use a cylindrical coordinate system with its origin in the center of the detector, where θ and ϕ are the polar and azimuthal angles, respectively, and pseudorapidity is $\eta = -\ln\tan(\theta/2)$. The missing E_T ($\vec{\not\!\!E}_T$) is defined by $\vec{\not\!\!E}_T = -\sum_i E_T^i n^i, i =$ calorimeter tower number, where n^i is a unit vector perpendicular to the beam axis and pointing at the i^{th} calorimeter tower. $\vec{\not\!\!E}_T$ is corrected for high- energy muons and also jet energy corrections. We define $\not\!\!E_T = |\vec{\not\!\!E}_T|$. The transverse momentum, p_T, is defined to be $p\sin\theta$.
[10] P. Dong, Ph.D. thesis, University of California at Los Angeles, 2008.
[11] T. Sjostrand, L. Lonnblad, S. Mrenna, and P. Skands, FERMILAB-PUB-03-457 (2003).
[12] J. Alwall *et al.*, J. High Energy Phys. 09 (2007) 028.
[13] M. Mangano, M. Moretti, F. Piccinini, R. Pittau, and A. Polosa, J. High Energy Phys. 07 (2003) 001.
[14] J. Alwall *et al.*, Eur. Phys. J. C **53** (2008), 473–500.
[15] M. L. Mangano, M. Moretti, F. Piccinini, and M. Treccani, J. High Energy Phys. 0701 (2007) 013.
[16] H. L. Lai *et al.* (CTEQ Collaboration), Eur. Phys. J. C **12** (2000), 375–392.
[17] A. Bhatti *et al.*, Nucl. Instrum. Methods Phys., Sect. A **566** (2006), 375–412.
[18] A. Abulencia *et al.* (CDF Collaboration), Phys. Rev. D **73** (2006), 032003.
[19] G. Corcella, I. Knowles, G. Marchesini, S. Moretti, K. Odagiri, P. Richardson, M. Seymour, and B. Webber, J. High Energy Phys. 01 (2001) 010.
[20] T. Aaltonen *et al.* (CDF Collaboration), Phys. Rev. D **77** (2008), 011108.
[21] N. Kidonakis and R. Vogt, Phys. Rev. D **78** (2008), 074005.
[22] M. Cacciari, S. Frixione, M. L. Mangano, P. Nason, and G. Ridolfi, J. High Energy Phys. 0809 (2008) 127.
[23] S. Moch and P. Uwer, Phys. Rev. D **78** (2008), 034003.
[24] V. Ahrens, A. Ferroglia, M. Neubert, B. D. Pecjak, and L. L. Yang, J. High Energy Phys. 1009 (2010) 097.